Experimental study of liquid-solid two phase flow over a step using PIV

E H Cando[1], X W Luo[1], V H Hidalgo[1], L Zhu[2] and A G Aguinaga[3]

[1] Department of Thermal Engineering, Tsinghua University, Beijing 100084, China
[2]China Institute of Water Resources and Hydropower Research (IWHR), Beijing 100038, China
[3]Department of Mechanical Engineering, Escuela Politécnica Nacional, Quito 17-01-2759, Ecuador

E-mail: luoxw@mail.tsinghua.edu.cn

Abstract. The present investigation focuses on the water-sand flow through a rectangular tunnel with a step using the Particle Image Velocimetry (PIV). Two cameras with appropriate optical filters have been used to capture each phase image separately. The optical filters were selected according to the optical properties of the sand and fluorescent tracers. Through data processing the experimental flow field such as the velocity profiles of sand and water had been obtained. In order to compare with the experiment, the steady state two phase flow fields were simulated using RANS method with k-ω SST turbulence model. It is noted that the numerical results matches the experimental results fairly good. Furthermore, the flow rates obtained from experimental and numerical velocity profiles also have a good match with the measurement by flow meter. The flow analysis shows that the water velocity variation induced by the presence of the step in the water-sand flow is equivalent to those cases with low sand concentration. However, the sand velocity in downstream region is 5% greater than the water velocity when the cross section is reduced in 25%.

Introduction

The dispersed phase flow in which one phase does not constitute a connected continuum is known as liquid-solid two phase flow [1]. It is encountered in various industries including energy generation, foods, pharmaceuticals, chemicals, etc. The flow through the hydraulic systems and its components (such as pump, turbine, pipeline, elbow, etc.) in places where the rivers have high sediment concentration produce the most erosive environments, resulting in high wear and short life to flow components, and leading problems like head and efficiency drop in hydraulic machinery. The wear prediction helps to improve the life of the components but requires the knowledge of the two phase-flows. Numerous experimental and numerical studies have been done; nevertheless the behaviour of the two phases and its interaction in the flow with different geometries has not been fully understood [2]. The flow velocity field, the interaction between two phases and the local particle concentration are considered to determine erosion coefficients [3]. A step is a geometry which is very similar to many structures in hydraulic systems, such as gap between the components of turbines and pumps, sudden

[1] Corresponding author. Tel.:+861062789853, Fax.:+861062785285
E-mail address: luoxw@tsinghua.edu.cn

variation sections in pipelines and geometries inside accessories; therefore the experimental flow velocity fields of continuous and disperse phases in this region allow to understand better the interaction between phases and establish data for numerical analysis.

The advanced and not-intrusive techniques for measuring flow velocity field are recommended because the intrusive measurement methods comprise the flow field by disturbing the flow [4].The most common non-intrusive and advanced technique used for velocity field measurements is particle image velocimetry (PIV) [3], which determine the instantaneous flow velocity field. In a single-phase flow condition, tracer particles are used inside the flow and a light sheet is used to illuminate. The velocity fields are calculated based on the particle images from the scattered light at different time. However, the PIV technique shows complications and challenges for two phases, due to simultaneous measurement, so that, images for each phase should be separated. Furthermore, PIV has one natural limitation which is the presence of phase boundaries in multiphase flows that blocks the optical path to the measurement location, which means that PIV can be used on low volume fractions of solid particles or gas-bubbles.

Due to the growth of industries which need to the transport fluid with solid concentration and the installation of hydroelectric power plant where the rivers have high sand concentration, there has been growing interest in liquid-solid two phase PIV techniques to measure two phase flow using PIV. Numerous solutions are proposed to measure two-phase flow using PIV. Hassan et al. [5] separated the phases using fluorescent particles and record the images with two cameras, both phases can be recorded in conjunction with filters to divide the signal and allow only the wavelength of the fluorescent light to pass. Khalitov and Longmire [3] used an algorithm to discriminated each phase, which is based on the intensity and the diameter of the appearing objects. Towers et al. [6] used a method that implied a laser pulse (λ = 532 nm) corresponding to the first image of PIV couples and laser pulse (λ = 610 nm) corresponding to the second image, it is note that fluorescent particles were used as tracer. A camera recorded single image from the two layers of the field-of view (FoV). Those images allow to separate the temporal information and to discriminate between the fluorescence and non- fluorescence. Rottenkolber et al. [7] used two techniques: First, the masking technique consisted of long-pass filters used in a camera, which reduces the scattering intensity level of the fluorescence emission. After, a binary mask by thresholding the image which preserves grey level was created. Finally some characteristics (size and shape) were deleted in the mask and filled using an average background grey level calculated from the original bitmap [8]. In the second technique, the properties of the correlations peaks were used to differentiate and separate the phases; for this technique is required a sufficient velocity different between the two phase flows which produce a double peak in the correlation plane. This technique is known as correlation peak. These techniques have been widely used for the two-phase flow PIV studies, some of which have been used to liquid-solid flow. Liu et al. [9] used a combination of PIV and image processing method to obtain the velocity information of the liquid-solid two phase flow in a chemical pump; this result show that the presence of the solid particles change the relative velocity of the liquid and the average relative velocity of mixture was larger than the clear water condition. Metha et al. [4] used the PIV in conjunction with refractive index matching to study the particulate flow in the impeller of a centrifugal pump, got the results of flow field at different particle concentration, and concluded that the highest particle velocity was near the suction side of the blade.

The application of the PIV technique to separate phases depends on study case. For liquid-solid two phase flow, all the above techniques could be used when the continuous phase is water and dispersed phase is sand. In this paper, the Hassan et al. [5] technique is used to simultaneous PIV of water-sand flow over a step when the sand concentration is low. Two cameras with appropriate optical filters are used to separate the liquid-solid phases. The first camera takes the images of tracers that represent the behavior of the continuous phase, and the second camera takes the images of second phase. For comparison, numerical simulation was also conducted to analyze the liquid-solid flow over the step.

Method and test rig

The experimental study aims to investigate the differences and similarities between the velocity of sand and water, when liquid-solid two phase flow through a changing section like a step. The close flow pump loop facility and PIV equipment (Figure 1) used in this research is located in China Institute of Water Resources and Hydropower Research. The flow passage components are built in stainless steel. However, the walls of the test section were performed in an optically clear material. The test section is constituted for a rectangle cross section of 80 x 20 mm and the localization of the step is shown in Figure 2. Water at 20° C is the carrier phase and the flow rate is 0.0087 m^3/s. The mixtures of solid and water are prepared in the tank.

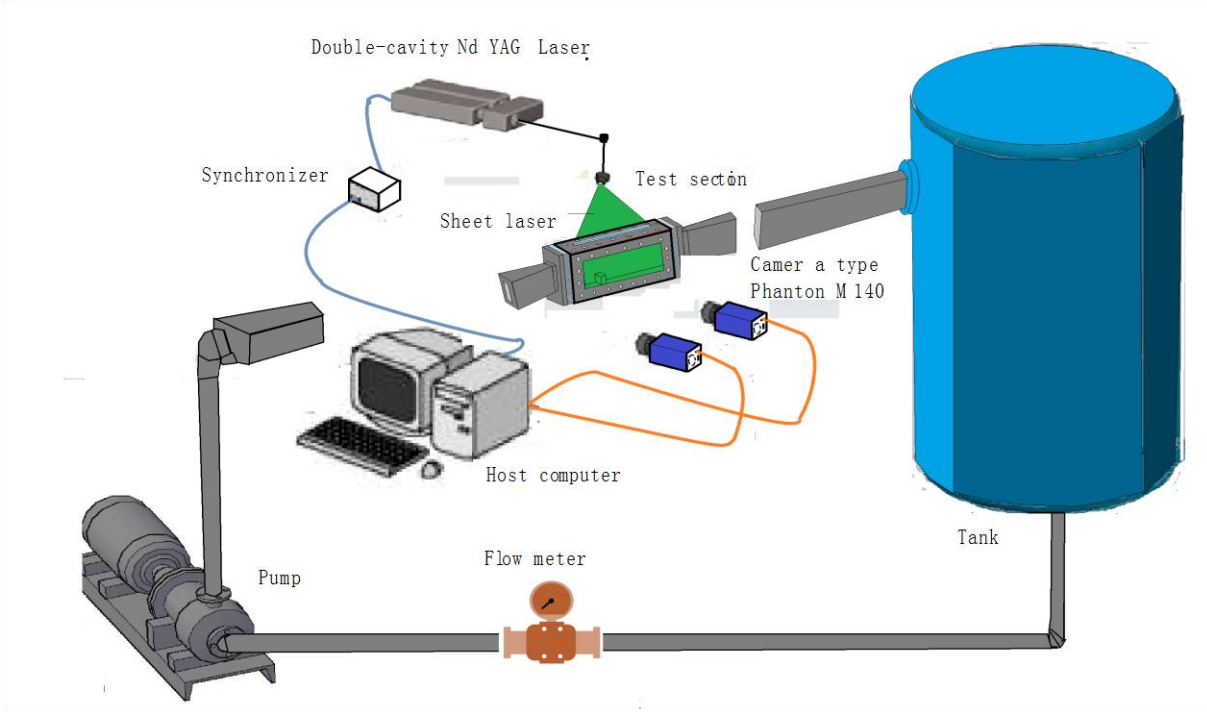

Figure 1. Experimental system.

The solid phase is sand particle with a bulk density of 2650 kg/m^3 with diameter of 20 μm. The volumetric particle concentration is less than 2% and it is assumed sand has a negligible effect on the flow of the carrier phase [1,10]. The tracers are the MMA fluorescence particles, whose diameter is 20 μm, the density is 1050 kg/m^3 and reflective index is 1.49.

1.1. PIV acquisition system

To perform a PIV test, the following equipment (Figure 1) are required: a 120 mJ/pulse Nd:YAG double-cavity laser (532 nm wavelength), laser light sheet optics, two camera Phantom M140, resolution: 2560 x 1600 pixels, a data acquisition system consisting of a PC, two camera filters and a frame grabber card . The laser beam is formed into a 1 mm thick light sheet using a combination of cylindrical and spherical lenses. The cameras focal axis is perpendicular to the plane of the laser light sheet to acquire flow images. Pair of single exposure image frames are required to enable cross correlation data processing. The image pair acquisition and processing is done using the DaVis software license version 8 offered by LaVision .The image pair acquisition is synchronized. The synchronization board and programmable timing unit are applied for image pair acquisition. The Δt used to take each pair of images was 100μs.

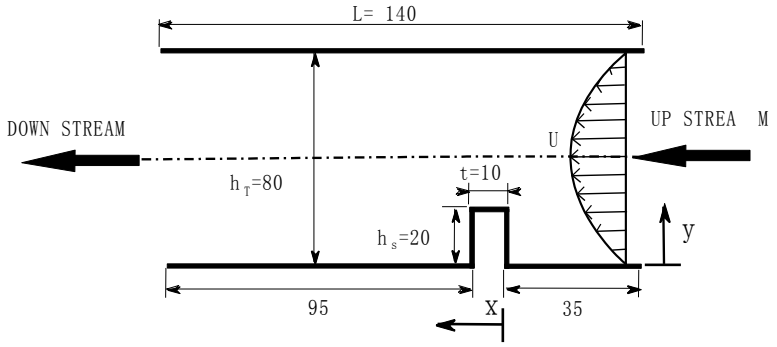

Figure 2. Illustration of test section (dimension in mm).

1.2. Description

The optical properties of the sand and the tracer have been used to separate images of each phase. The middle plane of flow through the test section is illuminated with the laser beam with 532 nm wavelength; this plane has a thickness of 1 mm. The first camera is equipped with an optical filter for LIF 540 nm cut, which takes the measurement of the tracers that represent behaviour of the continuous phase. This filter allows the passage only of light with a wavelength greater than 540 nm. For that reason this camera records only images of the tracers. On the other hand, the second camera has a filter 532 nm which blocks the passage of the light with a wavelength greater than 532 nm, therefore it records the flow of the sand. The geometry configuration of the PIV system is shown in Figure 3. The camera 1 is placed perpendicular to the plane of the object and the camera 2 is not completely perpendicular to the object plane; the position has a deviation of 5 degrees to the perpendicular plane but this deviation was evaluated and it does not affect the results. Finally a Rosemount vortex flow meter with 0.3% accuracy is used in the test rig for comparing the acquired data.

Numerical simulation

The numerical simulation in steady state has been carried out using the commercial software Ansys Fluent 14.0. The turbulence model used is Reynolds Average Navier Stokes (RANS *k*-ω SST) and it is considered that the dispersed phase has a negligible effect on the flow of water because the volumetric particle concentration is less than 2%, according with some authors [1,10].The conservation equations are based on the Eulerian approach for the water and the stochastic-Lagrangian approach for the particles [10-13]. The discrete phase model (DPM) is used to simulate the trajectory and particle velocity. This model can be used for these studies due to the sand low concentration [11].

1.3. Continuous Phase.

The continuity and momentum equations in steady state for continuous phase q (water) are expressed as:

$$\frac{\partial(\rho_q \overline{u_j})}{\partial x_j} = 0\,, \tag{1}$$

$$\frac{\partial(\rho_q \overline{u_j})}{\partial x_j} = -\frac{\partial \bar{P}}{\partial x_i} + \frac{\partial}{\partial x_j}\left(\mu \frac{\overline{\partial u_j}}{\partial x_j} - \rho_q \overline{u_i u_j}\right), \tag{2}$$

where ρ_q, u_j are the density and velocity, respectively. The term $-\rho_q \overline{u_i u_j}$ is the Reynolds stress.

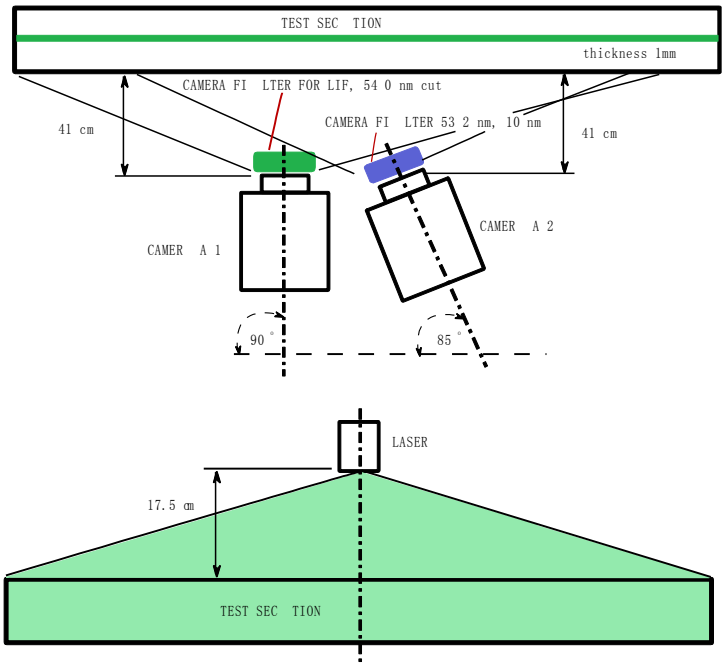

Figure 3. Camera, laser and optical filter positions.

1.4. Dispersed Phase.

DPM model is applied to calculate the trajectory and velocity of each particle injected based on Newton's second law of motion, which is given by Equation (3):

$$\frac{dv_i}{dt} = F_D + F_{pi} + F_{Bi} + F_{mi}, \tag{3}$$

where v_i is the particle velocity andF_D, F_{pi}, F_{Bi}, F_{mi} are the drag, pressure gradient, buoyancy and virtual mass forces, respectively. These forces are indicated from Equation (4) to (7).

$$F_D = \frac{\mu}{\rho_p {D_p}^2} . \frac{18 . C_D . Re}{24} (u_i - v_i), \tag{4}$$

$$F_{pi} = \left(\frac{\rho_f}{\rho_p}\right) v_i \frac{\partial u_i}{\partial x_i}, \tag{5}$$

$$F_{Bi} = \left(1 - \frac{\rho_f}{\rho_p}\right) g, \tag{6}$$

$$F_{mi} = \frac{-1}{2} \frac{\rho_f}{\rho_p} \frac{d}{dt} (u_i - v_i), \tag{7}$$

where$\mu\rho_p$, D_p, u_i, C_D and Re are dynamic viscosity, particle density, particle diameter, water velocity, drag coefficient and particle Reynolds number based on the relative velocity between the particle and fluid, respectively.

The drag coefficient $C_D$in Equation (4) is given by Equation (8):

$$C_D = \frac{24}{Re} . (1 + 0.15 . Re^{0.687}), \tag{8}$$

The Equation (5) is the force around the particle in the direction of the pressure gradient. The buoyancy force in Equation (6) is considered when the particle and fluid have significantly different densities and when the inclusion of gravitational effects is desired. The virtual mass force, Equation (7), accounts for the inertia of the fluid surrounding the particle.

Due to the flow characteristic, the following considerations also are applied: the particle-particle interaction and Brownian motion are neglected, the particle shape is considered as a spherical and the physical properties of the solid phase are constant.

Particle distribution was simulated with stochastic trajectory model in conjunction with the discrete random walk mode. The stochastic trajectory considers the fluctuations in the flow field, then the instantaneous value of the fluctuating flow velocity, u'_i(t), due to turbulence is included to predict the dispersion of particles. The instantaneous fluid velocity,$\overline{u_i} + u_i'(t)$, along the particle path is used to predict the turbulent dispersion of particle by the integrating the trajectory equations for each particle. The adequate number of particle injection is tracked repeatedly in order to generate a statistically meaningful sampling; the number of tries for this simulation was 10. Furthermore, the mass flow rate and exchange source terms for each injection are divided equally among multiple stochastic tracks. In the dispersed random walk model the interaction of a particle with a succession of discrete stylize fluid phase turbulent eddies is simulated by:

$$u'_i = \zeta\sqrt{\frac{2k}{3}}, \tag{9}$$

where k is the turbulent kinetic energy and ζis a normally distributed random number.

1.5. Geometry and solver

The computation domain is shown in Figure 4(a). The software Gambit has been used to generate a structured mesh, of which the mesh around the step is shown in Figure 4(b). The main mesh information is listed in Table 1.The mean calculated Yplus is 12.5.

The boundary conditions for this numerical simulation can be observed in Table 2.

The numerical solution is performed in double precision. The solution methods are: SIMPLE algorithm for pressure-velocity coupling and the second-order up wind spatial discretization have been used for the momentum equation, turbulence kinetic energy and specific dissipation rate. The residual reached of mass and momentum equations is 10^{-4}.

Results and discussions

Tests were conducted using two sand concentrations of 210 g/m^3 and 140 g/m^3. The experiment data processing of 200 pairs of PIV images for a selected area have been conducted. The PIV data were processed with an algorithm generated using Python and the results had been plotted using Tecplot 360. The numerical simulation has been carried out using ANSYS Fluent 14.0 and the data has been processed using ANSYS CFD Post 14.0. In the test, the height and width of a rectangle view are 140 mm and 80 mm, respectively. The selected area covers 60 mm over the step, i.e. 35 mm upstream and 95 mm downstream the step. The measurements were conducted at flow rate of 0.0087 m^3/s. The corresponding Reynolds number (based on the hydraulic diameter of the cross section) was 1.7 x 10^5 and average velocity U_m is calculated by U_m=Q/A, where Q and A are the flow rate and cross section area.

Table 1. Structural meshing.

Description	**Quantity**
Nodes	314128
Hexahedrons	233478

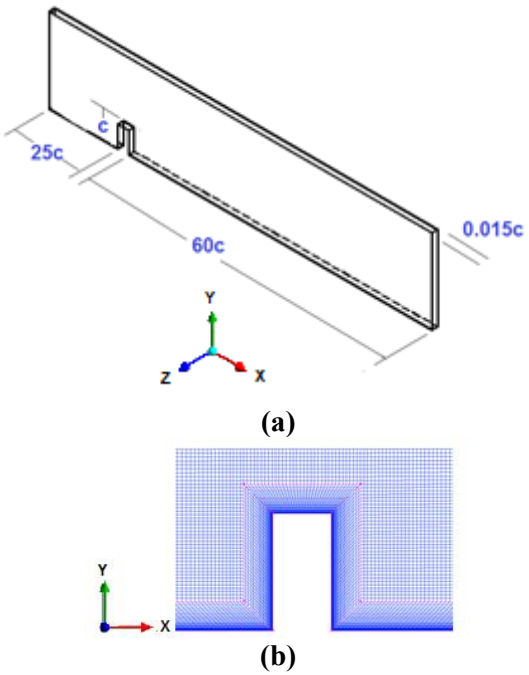

Figure 4. Domain and mesh: a) Computation domain; and b) Meshing around the step.

Table 2. Boundary conditions.

Surface	type	observation
Inlet	Velocity inlet	$U_\infty = 5.438\ m/s$
Outlet	Pressure outlet	
Top wall	Wall	No slip
Bottom wall	Wall	No slip
Side	Symmetry	

1.6. Validation

The numerical results with sand concentration of 210 g/m^3 have been compared with experimental results to validate the PIV technique. Moreover the flow rate calculated from velocity profiles is compare with the measurement of the flow meter. Figure 5 shows the FOV comparison between the experimental and numerical results, the velocity fields of numerical results for water are listed in the right column and the experimental results are listed in the left column. The experimental and numerical velocity profiles of each phase at x/L=0.4 are shown in the Figure 6. Finally, the calculated flow rate of numerical solution and PIV experimental results at x/L=0.4 are compared in the Table 3. The following milestones can be noted:

1) The water behavior has been obtained with good accurate using the fluorescent particles of density 1050 kg/m^3. It is supported because the PIV flow field velocity of water Figure 5(a) is reasonable match with numerical flow field velocity of water in Figure 5(b). Furthermore, the flow rate of the water obtained from experimental and numerical velocity profiles are similar to the flow meter measurement, as show in Table 3.

2) The velocity measurement of sand and water are successfully separated with the technique applied. The comparison between Figures 5(c) and 5(d) has a good match in the region where

the velocity is increased by the chance section. The comparison between experimental and numerical dimensionless profile at x/L=0.4 also shows the excellent match for the increased velocity of the sand due to the presence of step. Additionally, the flow rate obtained of the experimental water velocity profile at x/L=0.4 confirm that this camera takes the measurement only the tracers because the sand has higher velocity that should produce a higher flow rate.

3) The step inside of the geometry induces changes on the velocity profiles for both phases. However, the velocity increases in a different magnitude for sand and water, which is similar to previous studies liquid-solid two-phase flow [4,9].

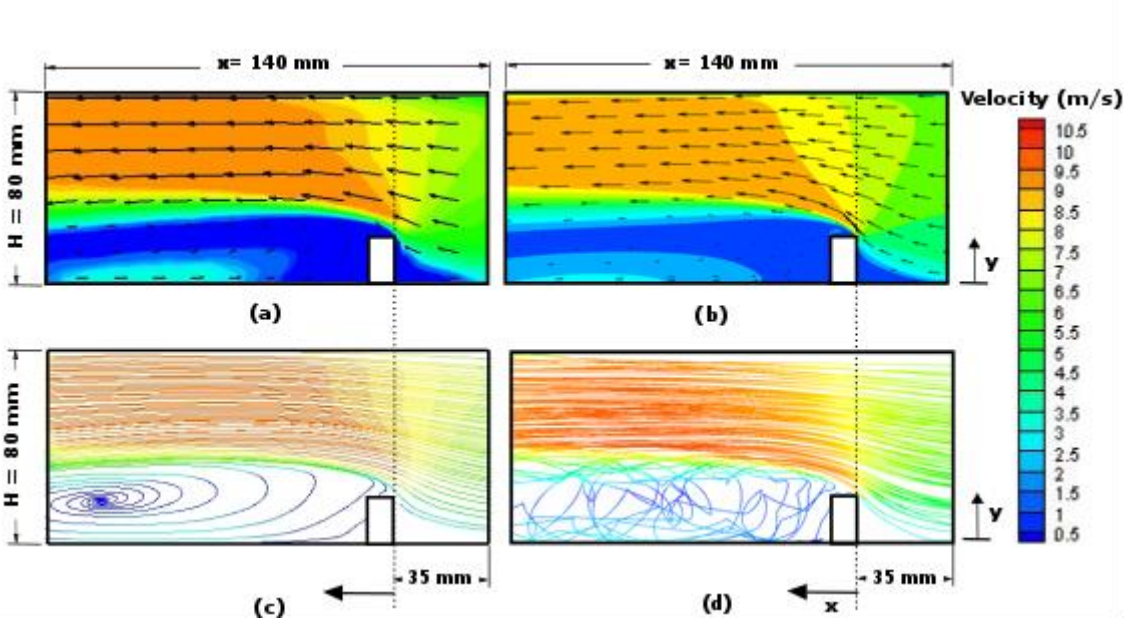

Figure 5. Experimental and numerical velocity fields with sand concentration of 210 g/m^3 and Re= 1.7 x 10^5.(a) Experimental water velocity plots, (b) Numerical water velocity plots, (c) Experimental sand velocity plots, and (d) Numerical sand velocity plots.

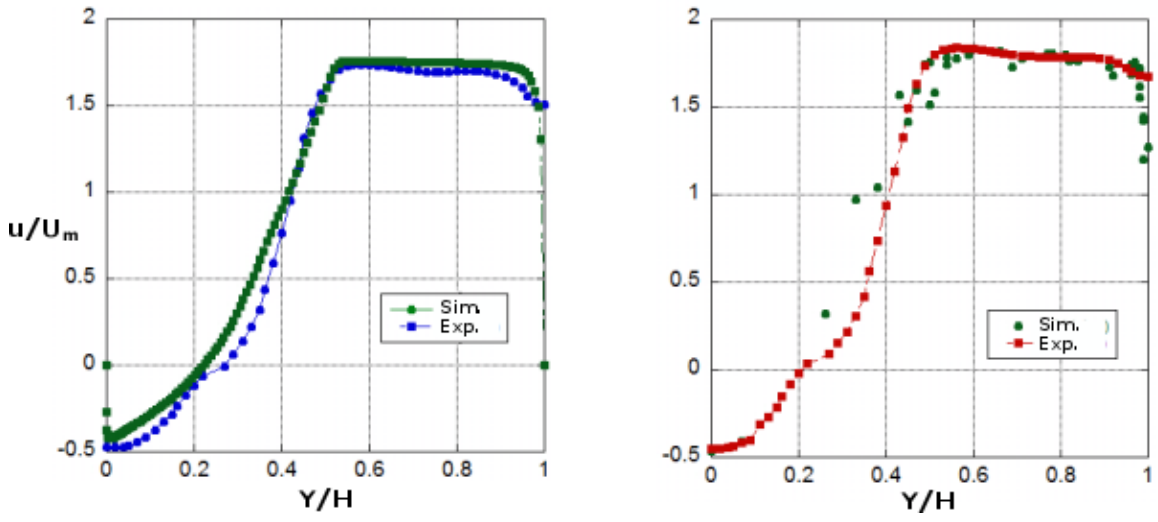

(a) (b)

Figure6. Experimental and numerical dimensionless velocity profiles at X/L=0.4, Re= 1.7 x 10^5. (a) Water and (b) Sand.

Table 3. Experimental and numerical comparison of flow rate.

Description	m^3/s	Abs error
Flow rate measurement	0.00870	–
Numerical profile	0.00864	0.67%
PIV profile	0.00843	3.1%

1.7. General feature

The changes of the velocity profiles obtained from experimental results are plotted in Figure 7 for both phases. Note that the dimensionless velocity, i.e. U/U_m is used to plot the velocity distribution. Both velocities of the sand and the water have similar profiles upstream. However, there is a difference close to the bottom, which can be the buoyancy force effects. In the same way, the velocity profiles change over the step and are higher than other regions due to channel reduction effects, but the magnitude of sand velocity is greater than water. Although the difference between the velocity of sand and water over the step is higher than in any other regions, the sand velocity remains greater than water downstream step.

Since the increased velocity of sand and water is different, it is necessary to study the velocity profiles after the step. Thus the Figure 8 show the experimental velocity profiles obtained by PIV at downstream step distance of x/L=0.4.

In order to evaluate whether a variation in the low concentration influences the velocity variation, the sand concentration of 140 g/m^3 was included in this analysis. The Figure 9 shows a comparison between dimensionless velocity profiles of sand and water with 140 g/m^3 and 210 g/m^3 sand concentration. These figures allow quantifying the increase in the sand velocity for two concentrations.

Based on these outcomes, the following can be described:

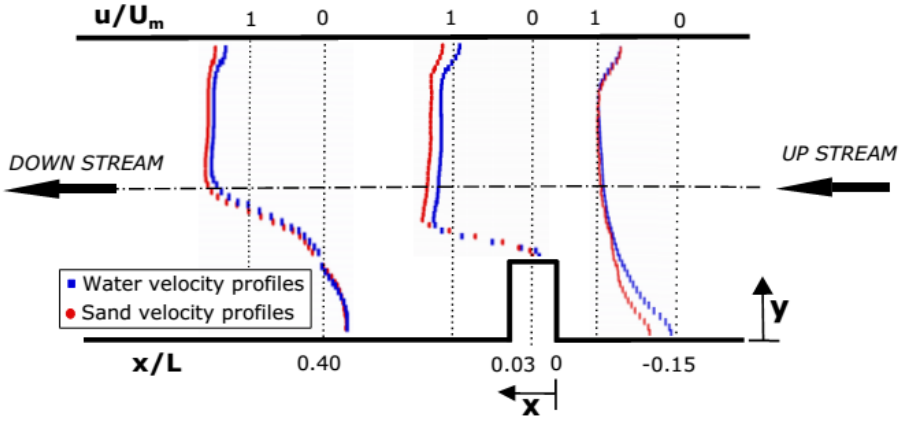

Figure 7. Dimensionless velocity profiles of water and sand, Re= 1.7 x 10^5.

1) The main characteristic of water flow field is the increase of velocity as the water approaches the step combined with large curvature in the streamlines. Furthermore the step downstream zone has a large region of recirculation flow.

2) The velocity profile of the water does not change for different low concentrations of sand, as shown in Figure 9(a)

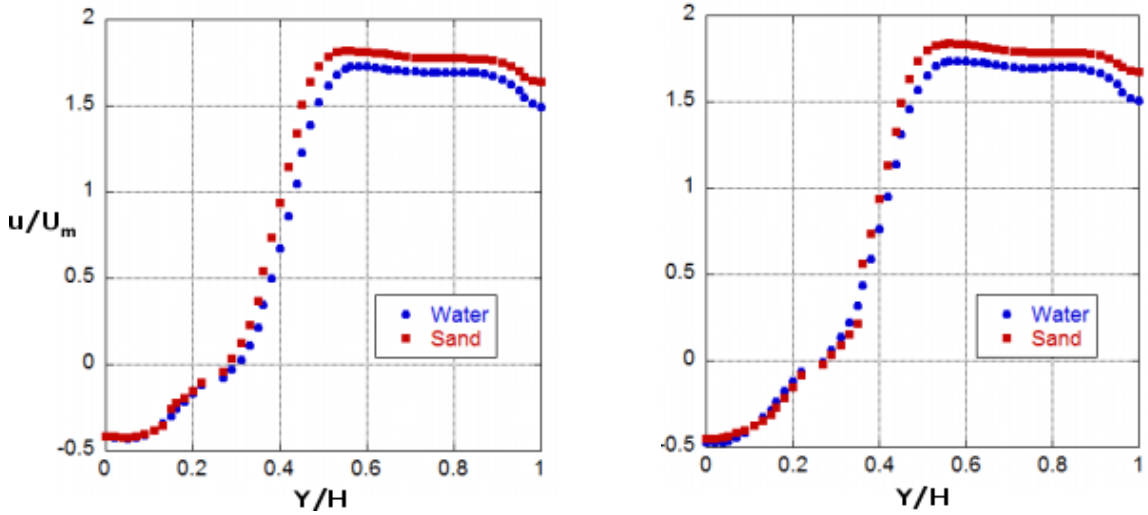

Figure 8. Dimensionless velocity profiles of sand and water at x/L=0.4and Re=1.7 x 10^5. (a) sand concentration of 140 g/m^3, and (b) sand concentration of 210 g/m^3.

3) In downstream step region, where the velocity increase occurs, the sand velocity increase 5% higher than water velocity, when the cross section is reduced in 25% and the sand velocity does not change for different low concentration.

Conclusions

The Particle Image Velocimetry (PIV) in conjunction with the simultaneous separation phase technique proposed by Hassan et al. [5] was successfully utilized to investigate the water-sand flow. Additionally, the following general conclusions can be obtained:

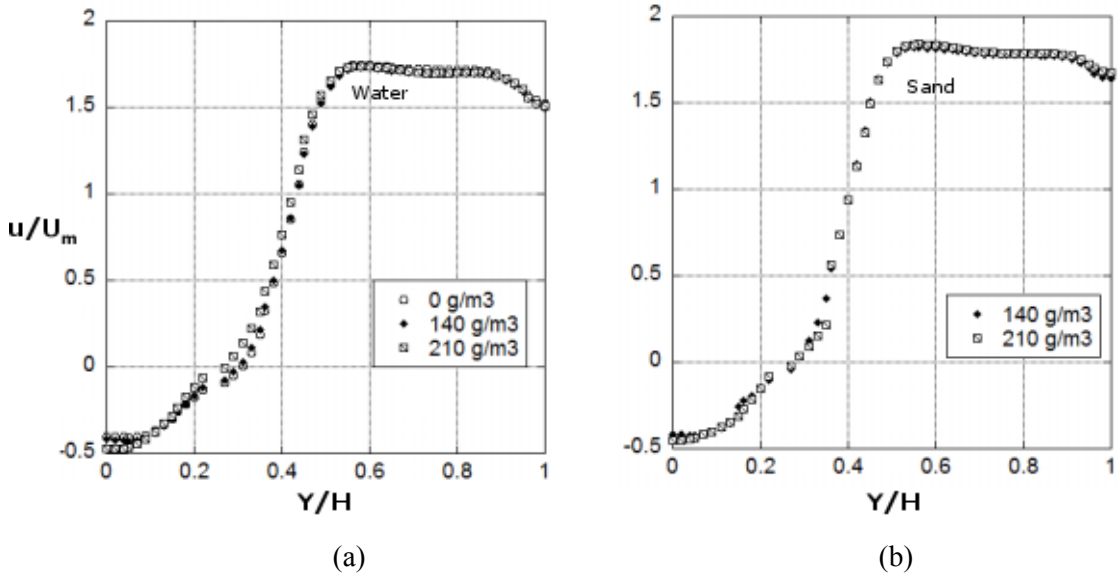

Figure 9. Dimensionless velocity profiles of water and sand at x/L=0.4, Re=1.7 x 10^5.

1. The particles with high density should not be used as tracers for PIV studies with changes in the cross section.
2. Downstream step, the velocity increase due to a change of section as a step is higher for sand than for water and is not influenced by low sand concentration variation.
3. The sand velocity is 5 % higher than water velocity for a reduction of 25% in the cross section and the water velocity profiles do not change due to variation of low concentrations of sand.

Acknowledgments
This work was financially supported by the Major National Scientific Instrument and Equipment Development Project (Project No. 2011YQ07004901), the National Natural Science Foundation of China (Project Nos. 51306018, 51406010 and 51179091) and State key Laboratory of Hydroscience and Engineering, Tsinghua University (Project Nos.2014-KY-05 and 2015-E-03).

References
[1] Crowe C T, Troutt, T R and Chung J N 1996 Two-phase turbulent flows, *Annu. Rev. Fluid. Mech.***28**1143
[2] Thapa B S, Dahlhaug O G and Thapa B 2015 Sediment erosion in hydro turbines and its effect on the flow around guide vanes of Francis turbine Renewable and Sustainable Energy Reviews **49** 1100–1113
[3] Khalitov D A and Longmire E K 2002 Simultaneous two-phase PIV by two-parameter phase discrimination Experiments in Fluids **32(2)** 252–268
[4] Mehta M, Kadambi J R, Sastry S, Wernet M, Addie G. and Visintainer R 2004 Study of particulate flow in the impeller of a slurry pump using PIVASME Heat Transfer/Fluids Engineering Summer Conferencevol1(North Carolina:USA) Paper No. HT-FED2004-56684 489-499
[5] Hassan Y A, Blanchat TK, Seeley C.H Jr., and Caanan, RE 1992 Simultaneous velocity measurements of both components of a two-phase flow using particle image velocimetry Int. J. Multiphase Flow **18 (3)** 371-395
[6] Towers D P, Towers C E, Buckberry C H and Reeves M 1999 A colour PIV system employing fluorescent particles for two-phase flow measurements. Measurement Science and Technology **10** 824–830
[7] Rottenkolber G, Gindele J, Raposo J, Dullenkopf K, Hentschel W, Wittig S, Spicher U and Merzkirch W 2002 Spray analysis of a gasoline direct injector by means of two-phase PIVExperiments in Fluids **32** 710–721
[8] Jakobsen M L, Easson W J, Created C A and Glass D H 1996 Particle image velocimetry: simultaneous two-phase flow measurement Meas. Sci. Tech. **7** 1270-1280
[9] Liu D and Yang M 2009 Research of liquid-solid two phase flow in the chemical pump. In Advances in Water Resources and Hydraulic Engineering 2203–2207
[10] Ji S M, Xiao F Q and Tan D P 2010 Analytical method for softness abrasive flow field based on discrete phase model Sci China Tech Sci. **53** 2867-2877
[11] Mostafa A.A. 1987 On the interaction of particles and turbulent fluid flow. Int. J Heat Mass Tran. **30 (12)** 2063–2075
[12] Okita R, Zhang Y. McLaury B S. and Shirazi S A 2012 Experimental and computational investigations to evaluate the effects of fluid viscosity and particle size on erosion damage. Journal of Fluids Engineering **134(6)** 061301
[13] Morsi S A and Alexander A J. 2006 An investigation of particle trajectories in two-phase flow systems Journal of Fluid Mechanics **55(02)** 193